Environmental and Climate Technologies
2026, vol. 30, no. 1, pp. 122–141
https://doi.org/10.2478/rtuect-2026-0009
https://content.sciendo.com

RIGA TECHNICAL UNIVERSITY

Efficiency of Heat Exchanger Systems Working with Nanofluids

Dagmara KOTRYS-DZIAŁAK[1*]

[1]*Department of Building Physics and Renewable Energy, Faculty of Environmental Engineering, Geomatics and Renewable Energy, Kielce University of Technology, Kielce, Poland*

Received 25.04.2025; accepted 05.12.2025

Abstract **– This paper presents a literature based comparative analysis of the heat transfer performance of heat exchanger systems operating with nanofluids. The study synthesizes and compares the results reported in published experimental and numerical works for different types of heat exchangers: shell and tube and plate heat exchangers. The comparison is based on key parameters including exergy efficiency η_{ex}, overall heat transfer coefficient *U*, and effectiveness ε. The results are presented as functions of the Reynolds number for laminar, transitional, and turbulent flow regimes, and for different types of nanofluids, including both mono and hybrid suspensions. The analysis shows that WC/DI nanofluids provide the highest overall heat transfer coefficient in plate heat exchangers with $U = 1110$ W/(m²K) at $Re = 525$, while 0.1 % Graphene/DI nanofluids achieve the best thermal performance in shell and tube heat exchangers exceeding *U* values of 0.4 % Fe_3O_4/DI:EG and 0.4 % ND/DI:EG by 85 W/(m²K) at $Re = 3000$. For plate heat exchangers 0.4 % ND/DI nanofluid demonstrate the highest effectiveness with ε equals to 62 % at $Re = 570$, whereas in shell and tube designs the best performance is obtained for 0.1 % GNP nanofluid with effectiveness reaching approximately 97.5 % at $Re = 500$. Furthermore, the Cu:ZnO/DI hybrid nanofluid achieved the highest exergy efficiency 66 % while other hybrid nanofluids exhibits exergy efficiencies lower by 31–34 % at a comparable Reynolds number. The results confirm the significant influence of nanofluid composition and Reynolds number in optimizing heat transfer efficiency.**

Keywords **– Effectiveness; exergy; plate heat exchanger; shell and tube heat exchanger.**

Nomenclature

Greek symbols

α	Heat transfer coefficient	W/(m²·K)
ε	Effectiveness	–
η	Efficiency	–
η_{ex}	Exergy efficiency	–
ρ	Density	kg/m³
φ	Nanoparticle volume concentration	%
θ	Temperature difference between two media	K
µ	Dynamic viscosity	Pa·s, (mPa·s)

*Corresponding author.
E-mail address: ddzialak@tu.kielce.pl

Dagmara KOTRYS-DZIAŁAK https://orcid.org/0000-0002-2539-403X

Latin symbols		
A	Heat exchange area	m^2
C	Heat capacity rate	W/K
C_p	Specific heat	kJ/(kg·K)
D_h	Hydraulic diameter	m
f	Friction factor	–
k	Thermal conductivity	W/(m·K)
$\dot{m}$	Mass flow rate	kg/s
NTU	Number of transfer units	–
Nu	Nusselt number	–
Q	Heat transfer rate	W
p	Pressure	Pa
Δp	Pressure drop	Pa
Re	Reynolds number	–
s	Entropy	J/(kg·K)
t	Wall thickness	m
T	Temperature	K
ΔT_{ln}	Logarithmic mean temperature	K
U	Overall heat transfer coefficient	$W/(m^2 \cdot K)$
Subscripts		
av	Average value	–
bf	Base fluid	–
c,i	Cold fluid at inlet	–
c,o	Cold fluid at outlet	–
h,i	Hot fluid at inlet	–
h,o	Hot fluid at outlet	–
i	Inlet	–
nf	Nanofluid	–
o	Outlet	–
th	Thermal value	–
Abbreviations		
CFD	Computational fluid dynamics	–
DI	Deionized water	–
DP	Double pipe	–
EG	Ethylene glycol	–
EO	Engine oil	–
GNP	Graphene nanoplatelets	–
HE	Heat exchanger	–
MWCNT	Multi-wall carbon nanotube	–

ND	Nanodiamond	–
PE	Performance index	–
PHE	Plate heat exchanger	–
S&T	Shell and tube heat exchanger	–
S&HC	Shell and helical-coil heat exchanger	–
TT	Twisted tape heat exchanger	–
WC	Tungsten carbide	–
vol.	Volume concentration	%

1. Introduction

Heat exchangers (HE) are devices designed to transfer thermal energy between two or more fluids at different temperatures [1]. Their construction enables the recovery of thermal energy and its reuse within a given system. These systems are used in many industrial sectors, including process, chemical, food, electronics, oil and gas industries [2]–[5]. In everyday life, they are most commonly found in household appliances such as refrigerators, radiators, and air conditioners [6], [7], as well as in domestic hot water systems installation with solar collector [8]. They also play a significant role in the aviation and automotive industries [2], [9], [10]. A wide range of working fluids can be applied in heat exchanger systems, with water, glycols, oils, and their mixtures being the most common [11]–[15]. The physical parameters of selected working fluids are presented in Table 1. Currently, efforts are focused on finding more efficient solutions that allow for intensification of heat exchange and improvement of the overall performance of installations. These include various types of nanofluids, which are suspensions with a dispersed phase composed of mineral particles of varying sizes from 0 to 100 nm [11], [16], [17]. The most commonly studied nanofluids contain a single type of nanoparticle with various shapes (e.g., spherical, nanowires). These include metallic particles such as gold (Au), silver (Ag), copper (Cu), titanium (Ti), iron (Fe), platinum (Pt) [18] as well as nonmetals, including oxides such as aluminum oxide (Al_2O_3), silicon dioxide (SiO_2), titanium dioxide (TiO_2), copper oxide (CuO), and carbon-based materials like graphene, carbon nanotubes (CNTs), multi-walled carbon nanotubes (MWCNT), single-walled carbon nanotubes (SWCNT) and diamond dust (ND) [19]. The local energy transformation described in [20] can be intensified by adding nanoparticles to the base fluids leading to an increase in the intensity of thermal-mass processes.

TABLE 1. THERMOPHYSICAL PROPERTIES OF SELECTED WORKING FLUIDS USED IN HEAT EXCHANGERS

Type of working fluid	**Temp., °C**	**Density ρ, kg/m³**	**Specific Heat C_p, kJ/(kg·K)**	**Thermal Conductivity *k*, W/(m·K)**
Water [21]	20	999	4.185	0.6
Ethylene glycol [21]	20	1126	2.354	0.256
Propylene glycol [21]	20	1035.3	2.479	0.1962
Ethylene glycol [22]	–	1115	2.664	0.26
Thermal oil Thermol 68 MOL [23]	20	880	1.87	0.132
Thermal oil Thermol 32 MOL [24]	20	872	1.88	0.133

Nanofluid production can be achieved through various methods. Some researchers use a two-step method, which involves mixing a base fluid with powdered nanoparticles (produced through physicochemical methods) using a stirrer and ultrasonication [25], [26]. Others employ physicochemical methods such as acetylene flame synthesis (AFS), electrical explosion wire (EEW), laser ablation, vacuum evaporation onto a running oil substance (VERSO), and submerged arc nanoparticle synthesis (SANS) [27]–[29]. In addition, nanoparticles obtained from natural sources are also used, such as bone powder, silicon nanoparticles, residual rice plants, and green tea leaves [30]. Hybrid nanofluids are also applied, combining at least two types of nanoparticles, mostly metallic and nonmetallic ones, such as Al_2O_3-Cu/DI, CuO-Cu/DI, Al_2O_3-Cu/DI, CNT-TiO_2/DI, MWCNTs-ZnO/SAE40, and others [31]–[34]. Table 2 presents example thermophysical properties of selected mono- and hybrid nanofluids commonly used in heat exchangers research (Table 2 in the Annex) [22], [35]–[41].

Despite the large number of studies on nanofluids and their interaction with heat exchangers, the reported results continue to vary in terms of the type of nanoparticles, their concentration, flow regime, and heat exchanger geometry. This work investigates how different nanofluids and their concentrations influence the energetic and exergetic performance of shell and tube and plate heat exchangers. The aim of this work is to present a literature-based comparative analysis of the performance of shell and tube and plate heat exchangers operating with nanofluids. The paper presents a synthesis of results from published experimental and numerical studies and compares selected key indicators of their performance: heat transfer coefficient, exergy efficiency, and effectiveness. The results are presented in the form of structured graphs, allowing for consistent comparison of nanofluid performance across different research works. The analysis made it possible to identify broader trends and relationships that were not addressed in the original studies. The author's contribution lies in organizing, classifying and evaluating literature data, providing a unified basis for assessing the performance of nanofluids in various heat exchangers.

The use of nanofluids in heat exchangers remains a highly topical research area. Due to the limited number of comprehensive research in this field providing clear results, a comparative analysis of various types of nanofluids, their concentrations, Reynolds number and efficiency parameter was undertaken. The difficulty lay in finding similar ranges and operating conditions for actual measurement systems, which significantly narrowed the scope of the review. The present work offers a systematic comparison of the most relevant and comparable studies available in the literature. The aim of this work is to indicate the need for further research in similar systems, which will contribute to more reliable conclusions regarding the energy and economic viability of using the discussed working fluids in thermal flow systems.

2. CONSTRUCTION AND CLASSIFICATION OF HEAT EXCHANGERS

Depending on the type of system and the heat exchanger employed, various types of nanofluids can be encountered. The first decision-making criterion is the construction of the heat exchanger. Heat exchangers are classified into three main groups: recuperators (membrane heat exchangers), regenerators, which use a storage material to transfer temperature between the fluids; and mixing-type exchangers, such as spray type condensers or cooling towers [42]. Alternatively, heat exchangers can also be categorized according to the flow arrangement of the working fluids as parallel-flow, counter-flow, cross-flow heat exchangers, or rotary heat exchangers that operate in ventilation systems. The classification of heating/cooling recovery systems is shown in Fig. 1.

The shell-and-tube heat exchanger and the plate heat exchanger belong to the group of recuperative heat exchangers; however, they differ in design, which affects their application and efficiency. Fig. 2 shows an example of a shell and tube heat exchanger operating in counterflow. It consists of a cylindrical shell and thin-walled tubes that form the heat transfer surface. It is most commonly constructed with one or two shells and can be single-pass, double-pass, or multi-pass. These types of heat exchangers are used primarily in industrial applications for high flow rates of steam or liquids. The shell and tube sides of a heat exchanger can be constructed from different materials. The high thermal conductivity of materials such as copper ensures effective heat transfer. These metals enhance heat exchange rates by facilitating the rapid transfer of thermal energy between fluids.

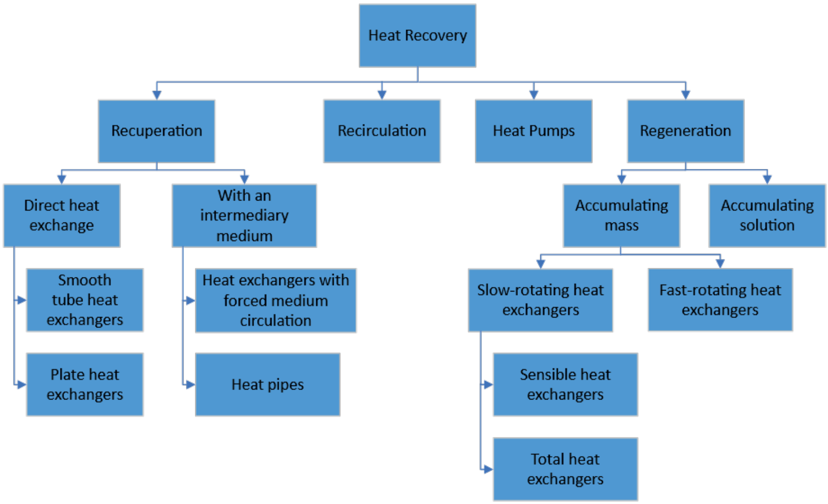

Fig. 1. Classification of heating/cooling recovery systems (based on [43]).

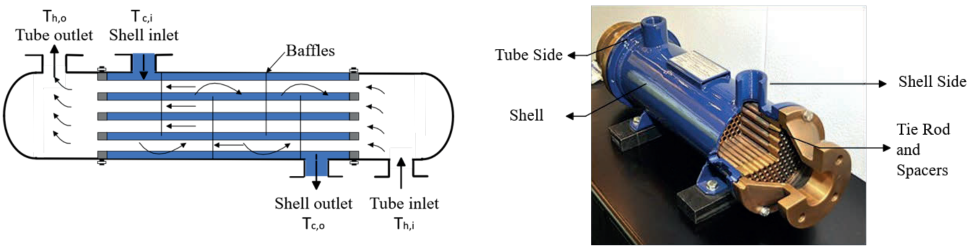

(a) (b)

Fig. 2. Shell and tube heat exchanger, counter–flow, single shell, single pass: a) cross–section of the heat exchanger, b) photograph of the actual system [44].

Plate heat exchangers are compact devices that consist of a series of thin plates to transfer heat between two fluids. Fig. 3 shows a plate heat exchanger and a photograph of a real system. These exchangers are manufactured as gasketed, brazed, welded, and semi-welded, with plate thicknesses ranging from 0.4 to 1.0 mm. The corrugated geometry of the plates increases the heat transfer surface area, which enhances heat transfer. The material selection for plate heat exchangers depends on the temperature and pressure of the heat transfer process, as well as the chemical composition of the fluids. Standard plates are often made of stainless steel or aluminium, while more specialized materials include acid–resistant steel, titanium, tantalum or nickel. Plate heat exchangers are highly versatile, allowing the addition or removal of plates to meet specific thermal requirements. They were first introduced in 1923 for milk pasteurization and have since been widely used in sectors such as chemical processing, petroleum, HVAC, refrigeration, dairy, pharmaceuticals, and food production.

Heat exchangers can also be classified on the basis of heat transfer mechanisms. Three basic mechanisms are distinguished: single-phase convection on both sides; single-phase convection on one side and two-phase convection on the other side, and two-phase convection on both sides. Fig. 4 illustrates the mechanisms mentioned above. In Fig. 4(b), fluid A undergoes evaporation, which means a two-phase flow, as it absorbs heat from fluid B, which remains in the same phase. In Fig. 4(c), fluid A undergoes condensation (phase change from gas to liquid), releasing heat to fluid B, which may change phase, for example, undergo boiling. Fig. 4(a) shows the mechanism where the fluid on both sides of the exchanger remains in the same phase, for example, liquid-liquid or gas-gas.

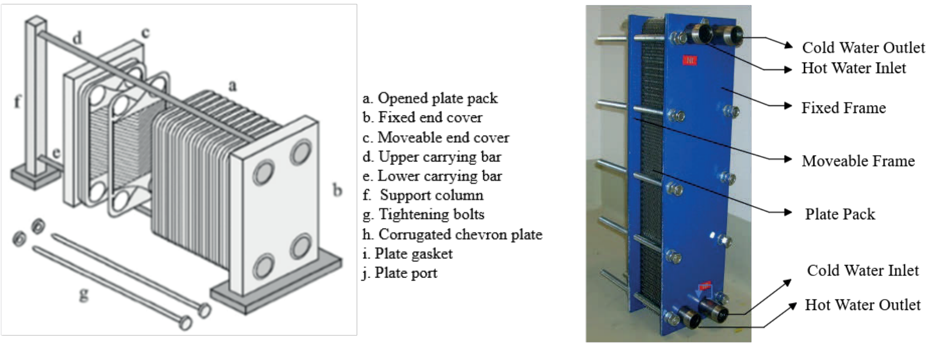

(a) (b)

Fig. 3. Plate heat exchanger: a) cross-section of the exchanger [45], b) photograph of the actual system [46].

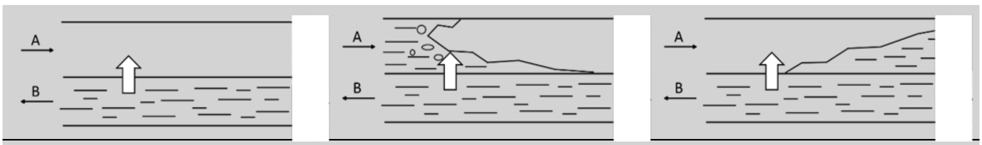

(a) (b) (c)

Fig. 4. Heat transfer mechanisms: a) single–phase, b) evaporation, and c) condensation.

The classification of heat exchangers is also based on the direction of fluid flow through the exchanger, which is defined as counter-flow, parallel-flow, and cross-flow. In parallel-flow heat exchangers, the two fluid streams enter together at one end of the heat exchanger and flow through it in the same direction, leaving at the same end. The reverse arrangement occurs in the counter-flow heat exchanger, where the two fluid streams flow in opposite directions. In the cross-flow arrangement, one fluid flows at a right angle to the flow path of the other fluid. Multiple flow arrangements are frequently used in heat exchanger designs, especially in shell and tube designs with different baffles. In the cross-flow heat exchangers, fluids may be mixed or unmixed. This depends on the design of the heat exchanger. When fluids flow through individual flow channels with no fluid mixing, the stream is called unmixed. When one fluid flows through individual flow channels (unmixed), while the other flows around the channels with the possibility of mixing, that steam is called mixed. Temperature distribution in a recuperative heat exchanger is presented in Fig. 5.

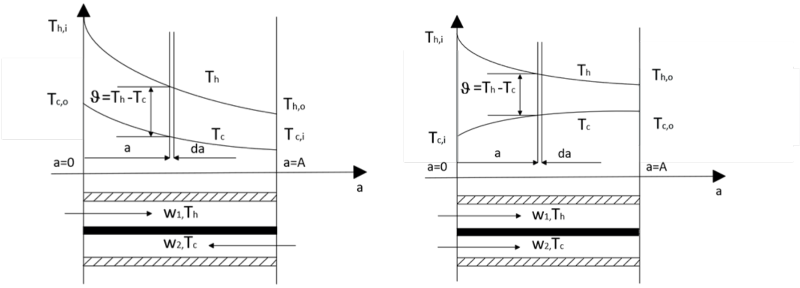

(a) (b)

Fig. 5. Temperature distribution in a recuperative heat exchanger: a) counter–flow, b) parallel–flow.

3. Effectiveness of Heat Exchangers Operating with Nanofluids

To evaluate the effectiveness of heat transfer in systems equipped with heat exchangers, several methods and key indicators are commonly used. These include the number of transfer units, *NTU*; effectiveness, ε; heat exchanger efficiency, η; entropy, *s*; exergy efficiency η_{ex}, overall heat transfer coefficient, *U*; fluid heat capacity, *C*; logarithmic mean temperature difference, $\Delta T_{\ln}$; and performance index, PE. Researchers around the world model these parameters numerically [47]–[49] and determine them indirectly through experimental methods [50]–[53].

Lazarevikj *et al.* [47] numerically analysed the performance improvement of a plate heat exchanger through which an Al_2O_3/water nanofluid flows in counter–flow at volume concentrations ranging from 0.5 % to 3 %. The working fluid, with an inlet temperature of T_i = 30 °C, was modelled at flow rates ranging from 1 to 4 L/min. The heating medium was water with a constant temperature of 70 °C and a flow rate of 3 L/min. The study demonstrated that the Al_2O_3/water nanofluid improves heat transfer, resulting in increases in the overall heat transfer coefficient, the heat transfer coefficient of the nanofluid, and the efficiency of the plate heat exchanger by 23 %, 30 %, and 12 %, respectively, compared to the base fluid (water). The overall heat transfer coefficient was found to increase with the nanofluid flow rate by up to 30 %. Graphite–based materials are commonly used for processes involving aggressive fluids, such as hydrochloric, sulfuric, or hydrofluoric acid, as well as chlorinated hydrocarbons or mining electrolytes. In swimming pool installations, where the water contains chlorine, fluorine compounds, and salts, titanium plates are typically used in gasketed exchangers.

In [52] Javadi *et al.* also analysed the impact of SiO_2, TiO_2, and Al_2O_3 nanoparticles as additives to the base fluid (water) in a plate heat exchanger. When comparing nanofluids with volume concentrations ranging from 0.2 % to 2 %, it was found that thermal conductivity, overall heat transfer coefficient, and heat transfer rate increased most significantly when Al_2O_3 was used. In this case, the maximum value of the overall heat transfer coefficient reached 309 W/(m²K) at a concentration of 0.2 %, which is 30 % higher compared to the SiO_2 nanofluid at the same concentration.

Cong Qi *et al.* [50] conducted experimental studies on heat transfer during the flow of a TiO_2/DI water nanofluid through double–tube (DT) heat exchangers with two different internal structures: smooth and corrugated tubes. The experimental conditions included nanofluid flow rates ranging from 1 to 5 L/min, mass concentrations from 0 to 0.5 %, and Reynolds numbers (*Re*) between 3000 and 12 000. The efficiency of the system increased with the nanofluid concentration. The convective heat transfer coefficient improved by 10.8 %, 13.4 %, and 14.8 % for concentrations of 0.1 %, 0.3 %, and 0.5 %, respectively. The number of transfer units (*NTU*) and effectiveness increased by 47.5 % and 11.4 %, respectively, compared to deionized water. The best results were achieved with the heat exchanger equipped with a corrugated inner tube; however, this design also resulted in a pressure drop that was, on average, 45 % higher than that of the smooth tube.

El-Maghlany *et al*. [51] investigated the performance of a horizontal double-tube heat exchanger operating with a CuO/DI water nanofluid. Their study reported a 16.5 % increase in system efficiency and an increase in the number of transfer units by up to 23.4 %. Nanoparticle volume concentrations were examined in the range of 1–3 %, with increments of 0.5 %, for Reynolds numbers between 2500 and 5000.

In [48], numerical studies were conducted on a square microchannel heat exchanger to evaluate the effects of four different nanofluids-aluminium oxide (Al_2O_3), silicon dioxide (SiO_2), silver (Ag), and titanium dioxide (TiO_2) – as well as Reynolds number and flow rate on heat flux density. It was observed that an increase in Reynolds number led to an increase in pumping power and a simultaneous decrease in efficiency. For example, at a higher flow rate of 2 % SiO_2 nanofluid with Re = 800, the exchanger performance improved by 25 % compared to the flow corresponding to Re = 100. Among the nanofluids analysed, the SiO_2 nanofluid was found to be the most effective, demonstrating approximately a 30 % improvement in heat transfer efficiency within the Reynolds number range of 100 to 800. The maximum pressure drop along the channels was minimal, measuring 5 %. Increasing the nanoparticle volume fraction from 2 % to 10 % resulted in a decrease in the PE for the SiO_2, Al_2O_3, and TiO_2 nanofluids by 16 %, 7 %, and 5 %, respectively. An exception was observed for the Ag nanofluid, where increasing the nanoparticle volume fraction to 6 % improved heat transfer performance by only 3 %.

As mentioned previously, significant indicators for assessing the efficiency of heat transfer in heat exchangers include exergy efficiency and total entropy. Rashidi *et al*. [54] conducted a comprehensive analysis of these metrics based on the most common type of heat exchanger, the shell and tube heat exchanger. The study showed that the temperature and mass flow rate of fluid streams in heat exchangers significantly influence entropy generation. Modifying the thermophysical properties of fluids reduces the entropy generation, thereby enhancing exergy efficiency. The study also examined the effects of physical parameters and nanoparticle structures on exergy and entropy. It was found that the shape of nanoparticles and/or the solid-phase concentration may be inversely proportional to entropy, while also contributing to increased exergy. Rashidi further analysed the impact of different baffle configurations on the performance of shell and tube heat exchangers. Four types of baffles were considered: conventional single-segmental baffle (CSSB), staggered single-segmental baffle (SSSB), flower segmental baffle (FSB), and hybrid segmental baffle (HSB). The heat exchanger equipped with HSB baffles exhibited the highest exergy efficiency, with this parameter being up to 38 % higher compared to the same exchanger with CSSB baffles. It should be noted that some researchers assess the thermal performance of nanofluids in heat exchangers using Nusselt number or friction factor. Mukherjee *et al*. [53] experimentally investigated a heat exchanger cooled by Al_2O_3:SiO_2/DI hybrid nanofluid (0.01–0.025 vol.%) under constant heat flux for Reynolds number between 6000 and 24 000. Their results, showing a 13.57 % increase in the average Nusselt number and a 10.08 % increase in the friction factor compared to water at the same *Re* number, confirm the potential of hybrid nanofluids to enhance convective heat transfer.

Currently, researchers are also looking for additional solutions to increase the efficiency of heat transfer by applying additional microstructures that can coat the surfaces of HE [55], [56]. Dąbek *et al.* [57] in their work analysed the use of phosphor bronze meshes that enhanced boiling intensity by increasing the number of active nucleation sites. Such solutions can also be applied to systems with heat exchangers to achieve more efficient operation. Bialek *et al.* [58] compared the use of microstructure coatings in the form of porous metal mesh and micro-ribs, and observed that heat fluxes can be more than eight times higher than on surfaces that are not covered with any coatings. This research shows that the use of different types of microstructures should be widely applied to equipment used in refrigeration or air conditioning [58].

4. ALGORITHM OF HEAT EXCHANGER EFFECTIVENESS

Heat exchange in recuperators can be either steady or transient. Transient heat exchange occurs at the beginning of operation or when the load of the recuperator changes. To determine heat transfer in a recuperator as simply as possible–in a tractable way, several simplifying assumptions are usually made: the specific heat of both fluids are constant, the overall heat transfer coefficient, *k,* is uniform over the entire heat transfer surface; there are no heat losses to the surroundings; and heat conduction in the exchanger wall (diaphragm) occurs only in the direction perpendicular to the flow. Fig. 5 illustrates the temperature distribution for two different fluid–flow configurations in the recuperative heat exchanger: counterflow in Fig. 5(a) and parallel-flow in Fig. 5(b), as discussed both in Section 2. The local temperatures of the fluids are denoted by T_h (hot fluid) and T_c (cold fluid). The subscript *'i'* refers to the inlet temperature, while the subscript 'o' denotes the outlet temperature. Knowing the values of the overall heat transfer coefficient *k*, as well as the inlet and outlet temperatures of both fluids, allows the heat transfer rate to be calculated, providing that the heat exchange area *A* is known. Conversely, if the heat transfer rate is known, the required area *A* can be determined. When comparing counter flow and co current flow under the same heat transfer coefficient *k* and heat transfer area *A*, the logarithmic mean temperature difference ΔT_{ln} between the hot and cold streams at the inlet and outlet can be expressed with Eq. (1):

$$\Delta T_{\text{ln}} = \frac{\theta_i - \theta_o}{\ln \frac{\theta_i}{\theta_o}}, \tag{1}$$

where θ_i and θ_o represents the temperature difference between two media exchanging heat at the inlet and outlet of the heat exchanger, respectively. The expressions for θ_i and θ_o differ for counter flow and co-current configurations and correspond directly to the temperature profiles shown in Fig. 5. The exact calculation formulas are shown in Fig. 6, which corresponds to Fig. 5. The ΔT_{ln} provides information on the intensity and effectiveness of the heat exchange process; a higher value of ΔT_{ln} indicates more intensive heat exchange between the streams. The maximum heat transfer coefficient is observed at the heat exchanger inlet. At the outlet, the fluid temperatures approach each other, as shown in Fig. 5(a) and 5(b). Counter–flow heat exchangers in Fig. 5(a) are characterised by higher thermal effectiveness compared to parallel-flow heat exchangers in Fig. 5(b) primary due to the higher value of the logarithmic mean temperature difference for a given set of operating conditions. The calculation of the logarithmic temperature difference therefore differs for parallel-flow and counter–flow, and this distinction is reflected in the computational algorithm used to evaluate the effectiveness of heat exchange devices.

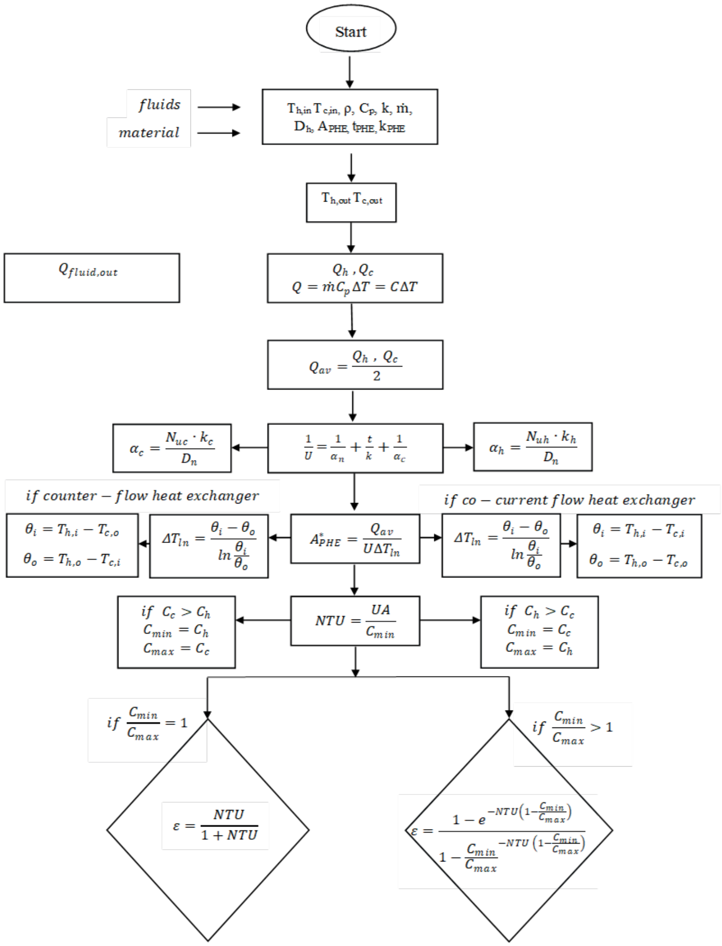

Fig. 6. Algorithm to calculate the efficiency of shell and tube and plate heat exchangers working with nanofluids when the heat transfer surface is known (author's own work).

Based on the relationships described above, the step-by-step procedure for calculating the effectiveness of shell and tube and plate heat exchangers is presented in Fig. 6. The algorithm was developed by the author as a synthesis of the calculation steps commonly used for evaluating heat exchanger performance. The indicators appearing in the algorithm, which quantify the effectiveness of heat exchange involving nanofluids are analysed later in this article (see Section 5).

5. Discussion of Heat Transfer Characteristics in Nanofluid-Based Heat Exchangers

In this section, a detailed analysis of the collected literature data is presented for the overall heat transfer coefficient, effectiveness, and exergy efficiency of the two most common types of heat exchangers: shell and tube and plate heat exchanger. The analysis was carried out using selected nanofluids over various Reynolds number ranges, both for laminar and turbulent flows. All figures presented in this section were created by the author and based on numerical and experimental data reported in the reviewed literature.

The average overall total heat transfer coefficient, related to heat transfer area *A*, as a function of the type of heat exchanger, is shown in Figs. 7–9. Fig. 7 illustrates how the type and concentration of nanofluid affect heat transfer in a shell and tube heat exchanger system. The most efficient nanofluid in this comparison is the 0.1 % Graphene/DI suspension [59]. The overall heat transfer coefficient *U* for this nanofluid increases by 75 % in the Reynolds number range from 500 to 3000, which increases by 11 % for each unit of *Re* number. In contrast, the *U* value for ND/DI:EG [60] and Fe_3O_4/DI:EG [61] nanofluids are comparable and remain almost constant in the Re range of 1250 to 4000 and at approximately 225 W/(m^2K). In the laminar range, 0.3 % Al_2O_3/DI [62] and 0.5 % SiO_2/DI [63] nanofluids flowing through the shell and tube exchanger achieve significantly better heat transfer performance, the *U* factor clearly increases with increasing flow velocity, with an average increase of 10 % per each unit of *Re* number.

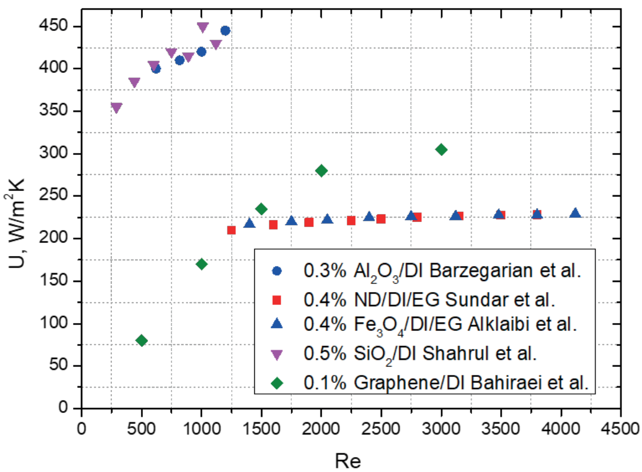

Fig. 7. Overall heat transfer coefficient for shell and tube HE and *Re* < 4500. Data compiled by the author based on: 0.3 % Al_2O_3/DI [62], 0.4 % ND/DI/EG [60], 0.4 % Fe_3O_4/DI/EG [61], 0.5 % SiO_2/DI [63], 0.1 % Graphene/DI [59].

The influence of other nanofluids operating in shell and tube heat exchanger at significantly higher Reynolds number is presented in Fig. 8. The nanofluids considered are: 0.5 % MWCNTs/DI [64], 0.2 % Al_2O_3/DI [65] and, for comparison, Molten Salt [66]. It was observed that Molten Salt achieved the highest value of the overall heat transfer coefficient, although it was tested over a relatively narrow Reynolds number range from 5000 to 7000. For *Re* = 7000, which is the upper limit of the tested range, Molten Salt reached a heat transfer coefficient of 660 W/(m^2K), i.e., 137 % higher than that of Al_2O_3/DI nanofluid. In the Reynolds number range of 2500 to 12 500 for the 0.5 % MWCNTs/DI and 0.2 % Al_2O_3/DI nanofluids, the overall heat transfer coefficient *U* was found to be 1.2 times higher for 0.2 % Al_2O_3/DI compared to 0.5 % MWCNTs/DI. In this case, the *U* increased by 6.9 % and 8.3 % per 1000 Re for 0.5 % MWCNTs/DI and 0.2 % Al_2O_3/DI, respectively.

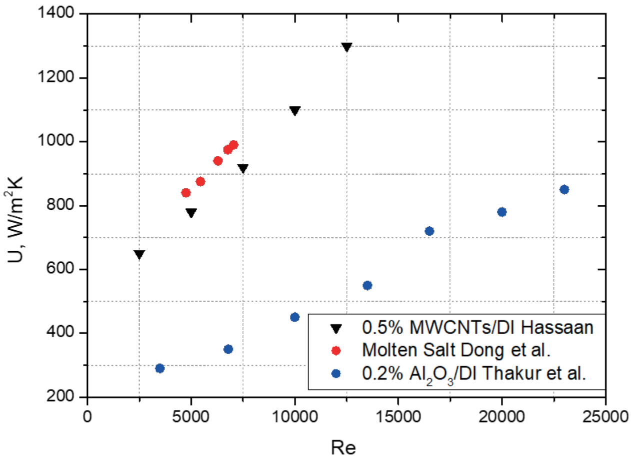

Fig. 8. Overall heat transfer coefficient for shell and tube HE and *Re* < 25 000. Data compiled by the author based on: 0.5 % MWCNTs/DI [64], Molten Salt [66], 0.2 % Al_2O_3/DI [65].

Fig. 9 presents the overall heat transfer coefficient for laminar flow, with the maximum Reynolds number equal to 700, considering six different nanofluids. Among them, the highest value of the heat transfer coefficient *U* was achieved by the WC/DI nanofluid [67], with a maximum *U* of 1110 W/(m²K) at *Re* = 525. The lowest value was observed for the 0.6 % Fe_3O_4:SiO_2/DI hybrid nanofluid [68], which reached a maximum *U* of 550 W/(m²K) at *Re* = 280, i.e., half the value obtained for the tungsten carbide nanofluid (WC/DI). Similar values of *U* were recorded for 0.4 % ND/DI [69], 0.3 % Fe_3O_4:MWCNT/DI [70], and 0.6 % Fe_3O_4:SiO_2/DI, which increased by 47.06 %, 38.18 % and 35.45 %, respectively, within the studied Reynolds number range. This corresponds to an increase of 0.11 %, 0.10 % and 0.09 % per unit increase in *Re*, respectively.

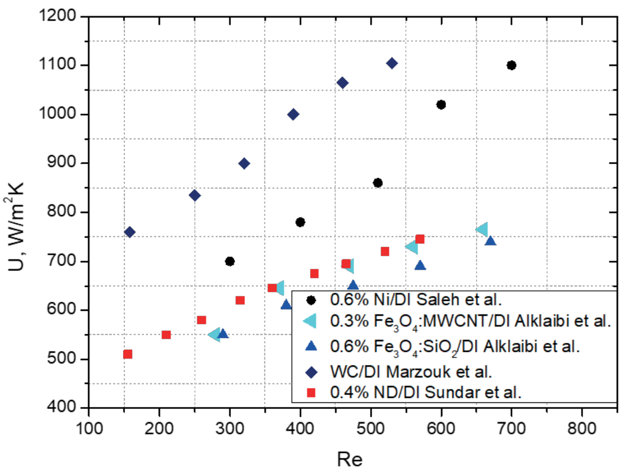

Fig. 9. Overall heat transfer coefficient for Plate HE and *Re* < 800. Data compiled by the author based on: 0.6 % Ni/DI [71], 0.3 % Fe_3O_4:MWCNT/DI [70], 0.6 % Fe_3O_4:SiO_2/DI [68], WC/DI [67], 0.4 % ND/DI [69].

Fig. 10 and Fig. 11 show the dependence of the exergetic efficiency as a function of the Reynolds number for laminar flow in a plate heat exchanger, and for turbulent flow in a shell and tube heat exchanger, respectively. The highest exergetic efficiency was achieved by the plate heat exchanger, reaching 74 % at *Re* = 650 for the 0.3 % MWCNT:Fe_3O_4/DI hybrid nanofluid [70]. The 0.4 % ND/DI [69] and 0.3 % MWCNT:Fe_3O_4/DI nanofluids [70] in the Reynolds number range from 300 to 560 exhibits similar exergetic efficiencies, increasing from 46 % to 74 %. The 0.3 % Ni/DI [71] nanofluid achieves lower efficiencies in this range, oscillating between 40 % and 67 %.

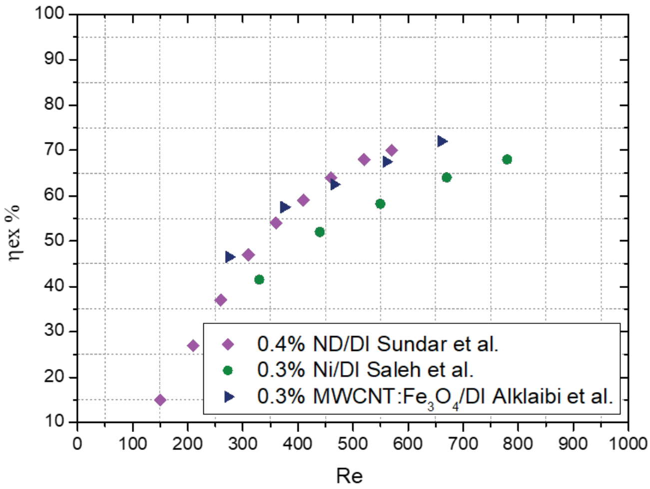

Fig. 10. Exergy for Plate HE and *Re* < 1000. Data compiled by the author based on: 0.4 % ND/DI [69], 0.3 % Ni/DI [71], 0.3 % MWCNT: Fe_3O_4/DI [70].

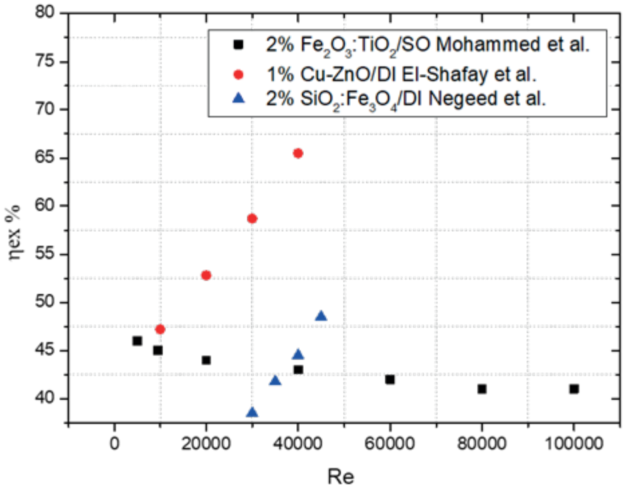

Fig. 11. Exergy for Shell and Tube HE and *Re* < 100 000. Data compiled by the author based on: 2 % Fe_2O_3:TiO_2/SO [72], 1 % Cu:ZnO/DI [73], 2 % SiO_2:Fe_3O_4/DI [74].

The exergetic efficiency of the shell and tube heat exchanger in the *Re* range of 7000 to 100 000 shows no clear correlation between the type of nanofluids tested. In all three cases, the volume concentration of nanoparticles is 1 % or 2 % and the working fluids are hybrid nanofluids. The highest exergetic efficiency equal to 65 %, was obtained for a 1 % Cu:ZnO/DI solution [73] at *Re* = 40 000, with the efficiency increasing by 6.17 % for every 10 000 increase in *Re*. For a 2 % SiO_2:Fe_3O_4/DI nanofluid [74], the exergetic efficiency increases by about 10.56 % for every 10 000 *Re*. In contrast, for 2 % Fe_2O_3:TiO/SO [72], as the Reynolds number increases from 5000 to 100 000, the exergetic efficiency decreases from 46.5 % to 40.5 %.

The next set of graphs, shown in Fig. 12 and Fig. 13, presents the effectiveness of the two types of heat exchangers. A linear increase in effectiveness was observed in [69] and [70], where two nanofluids were studied: 0.4 % ND/DI and a 0.3 % hybrid MWCNT:FeO_3/DI. Higher effectiveness of the plate heat exchanger was obtained for 0.4 % ND/DI; the value of this parameter increased to 62 % from the value of 42 % in the Reynolds number range from 150 to 570. The total increase in the heat transfer effectiveness was 20 %, which corresponds to approximately 0.0476 % per unit increase in *Re* number. The highest effectiveness equal to 97.5 % was obtained for the shell and tube heat exchanger operating with 0.1 % GNP [59] and *Re* = 500. The effectiveness values for 0.4 % ND/EG:DI [60] and 0.4 % Fe_3O_4/EG:DI [61] are similar in the Reynolds range from 1250 to 4100: for 0.4 % ND/EG:DI they range from 47.5 % to 52.5 %, and for 0.4 % Fe_3O_4/EG:DI from 49 % to 51 %. The 0.1 % Al_2O_3 nanofluid [75] was tested in laminar flow up to *Re* = 750, with effectiveness value decreasing from 55 % to 45 %. The lowest effectiveness was observed in [51] for the highest testes concentration of 1 % Cu/DI, with a maximum value of 37.5 % at *Re* = 4500, as shown in Fig. 13.

In addition to the graphical comparison presented in Figs. 7–13, the most important literature-based data are summarized in Table 3 in Annex [51], [59]–[75]. This table includes the type of nanofluid and its volume concentration, the heat exchanger configuration, the Reynolds number range, the overall heat transfer coefficient, (including the ratio U_{nf} / U_{bf}) as well as effectiveness and exergy efficiency. Table 3 also contains information in relation to quality of underlying data. The last column reports the uncertainty analysis for the measuring instruments and, where available, the propagated uncertainties of the calculated parameters (*Re*, *Nu*, *U*, ε, η_{ex}). This additional information highlights that not all experiments and simulations provide the same level of metrological detail. Furthermore, Table 3 also reinforces the trend discussed in this section. For Shell and tube heat exchanger most nanofluids 0.5 % MWCNT/DI, 0.3 % Al_2O_3/DI, 0.1 % Graphene/DI show a clear increase in the overall heat transfer coefficient compared to the base fluid which corresponds to the behaviour illustrated in Fig. 7 and Fig. 8. For plate heat exchangers operating in the laminar flow, the table confirms the high values of *U*, effectiveness and exergetic efficiency obtained for nanofluid 0.4 % ND/DI, WC/DI and hybrid 0.3 % Fe_3O_4:MWCNT/DI in agreement with Figs. 9 –12.

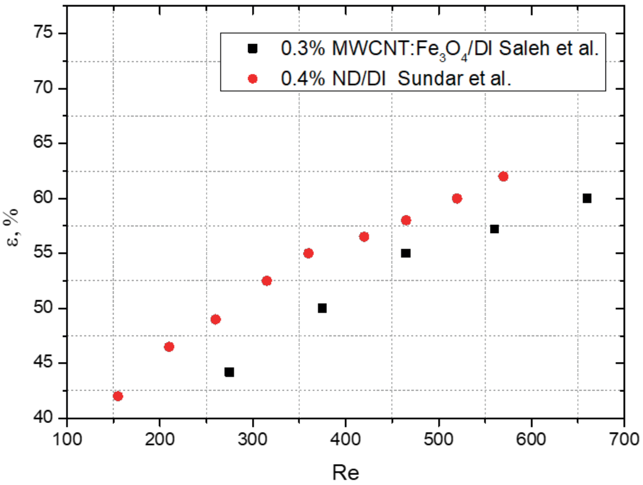

Fig. 12. Effectiveness for Plate HE and *Re* < 700. Data compiled by the author based on: 0.3 % MWCNT:Fe_3O_4/DI [70], 0.4 % ND/DI [69].

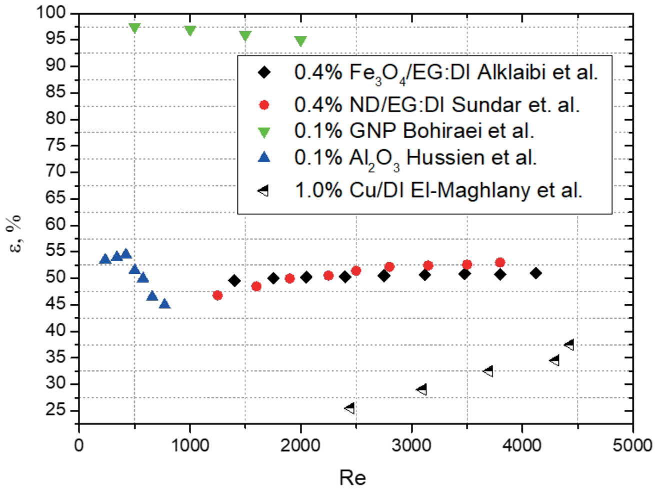

Fig. 13. Effectiveness for Shell and Tube HE and *Re* < 5000. Data compiled by the author based on: 0.4 % Fe_3O_4/EG:DI [61], 0.4 % ND/EG:DI [60], 0.1 % GNP [59], 0.1 % Al_2O_3 [75], 1.0 % Cu/DI [51].

6. Conclusions

The article presents an algorithm for calculating the efficiency of shell and tube and plate heat exchangers, which enables the assessment of how the thermodynamic parameters of the working medium influence the overall efficiency of the system. The analysis confirms that both the thermal conductivity of the nanofluid and also the hydraulic conditions represented by the Reynolds number have a decisive influence on the final energy effect of the exchanger of a given type. Based on the comparative analysis performed by the author using data from the most current publications related to the study, the following conclusions can be drawn:

- In PHE operating in the laminar regime, the highest overall heat transfer coefficient was obtained for the WC/DI nanofluid, (U_{max} = 1110 W/(m^{2}K) for *Re* = 525).
- Analysis of the heat transfer coefficient for shell and tube heat exchangers at Reynolds number < 1250 showed that the results of the two tested nanofluids – 0.5 % SiO_2/DI and 0.3 % Al_2O_3/DI are comparable, with a maximum of 450 W/(m^{2}K) for the 0.5 % SiO_2/DI nanofluid.
- In Reynolds number range 1250–3000, in the analysed shell and tube heat exchangers, the highest overall heat transfer coefficient was achieved by 0.1 % Graphene/DI nanofluid, exceeding the values obtained for 0.4 % Fe_3/DI/EG and 0.4 % ND/DI/EG by 85 W/(m^{2}K) at *Re* = 3000.
- Very limited data are available in the literature for the effectiveness ε of plate heat exchangers. From the analysed studies, ε ranged 40–62 % for 0.4 % ND/DI and 0.3 % MWCNT:Fe_3O_4/DI nanofluids, with the highest value ε = 62 % achieved for 0.4 % ND/DI and *Re* = 570.
- For shell and tube heat exchangers, the highest effectiveness ε was obtained for 0.1 % GNP nanofluid (97.5 % at *Re* = 500). Within the analysed *Re* range (500÷2000), ε values for 0.1 % GNP were approximately 44 % higher than those of 0.4 % ND/EG:DI and 0.4 % Fe_3O_4/ED:DI at *Re* = 2000.
- Exergetic efficiency η_{ex} strongly depends on the type of nanoparticle. The highest value 65.5 % was achieved for a hybrid Cu:ZnO/DI nanofluid. The exergy efficiency reported is also related to the use of a circular tube equipped with helical twisted tape. At *Re* = 40 000, η_{ex} is lower by 31 % and 34 % for SiO_2:Fe_3O_4/DI and Fe_3O_4:TiO_2/SO nanofluids, respectively.

The comparative analysis presented in this paper shows how various nanofluids can increase the overall heat transfer coefficient, exergy efficiency, and the effectiveness of both shell and tube and plate heat exchangers. Such improvements can reduce the size of heat exchangers, but also lower the medium temperature difference between the supply and return, and consequently reduce the consumption of electricity or fuel used in the system. Such a conclusion was reported by Wciślik and Taler [49] whose research focused on plate heat exchanger used in solar installation and showed that using TiO_2:SiO_2/EG nanofluid instead of solar liquid can increase exergy efficiency and contribute to energy savings under economically feasible operating conditions. However, the benefits of using nanofluids as working fluids are offset by the additional pressure loss generated by the system, higher pumping power [49] as well as problems related to the long–term stability, preparation, and environmental impact of nano additives production, use and disposal. Understanding electrokinetic properties such as zeta potential is crucial for controlling aggregation and stability of dispersed phase, which is consistent with [76] in other complex colloidal system. Therefore, further experimental and numerical research is important to determine whether the increased heat transfer efficiency justifies the environmental costs [77].

ANNEX

Available: https://zenodo.org/records/18460283

REFERENCES

[1] Hajatzadeh Pordanjani A., Aghakhani S., Afrand M., Mahmoudi B., Mahian O., Wongwises S. An updated review on application of nanofluids in heat exchangers for saving energy. *Energy Conversion and Management* 2019:198:111886. https://doi.org/10.1016/j.enconman.2019.111886

[2] Zheng Z., Pei X., Wang Y., Hou L. Pressure Effect on the Surface Deposition of Aviation Fuel in a Heat Exchange Tube. *Energies (Basel)* 2022:15(18). https://doi.org/10.3390/en15186770

[3] Jafari S. M., Saramnejad F., Dehnad D. Designing and application of a shell and tube heat exchanger for nanofluid thermal processing of liquid food products. *J Food Process Engineering* 2018:41(3):e12658. https://doi.org/10.1111/jfpe.12658

[4] Arsenyeva O., Tovazhnyanskyy L., Kapustenko P., Klemeš J. J., Varbanov P. S. Review of Developments in Plate Heat Exchanger Heat Transfer Enhancement for Single-Phase Applications in Process Industries. *Energies* 2023:16(13):4976. https://doi.org/10.3390/en16134976

[5] Dekhil M. A., Simo Tala J. V., Bulliard-Sauret O., Bougeard D. Development of an innovative heat exchanger for sensible heat storage in agro-food industry. *Appl Therm Eng* 2020:177:115412. https://doi.org/10.1016/j.applthermaleng.2020.115412

[6] Tang F., Nowamooz H. Factors influencing the performance of shallow Borehole Heat Exchanger. *Energy Convers Manag* 2019:181:571–583. https://doi.org/10.1016/j.enconman.2018.12.044

[7] Kayaci N. *et al.* Experimental and numerical investigation of ground heat exchangers in the building foundation. *Energy Convers Manag* 2019:188:162–176. https://doi.org/10.1016/j.enconman.2019.03.032

[8] Wciślik S. The Influence of Nusselt Correlation on Exergy Efficiency of a Plate Heat Exchanger Operating with TiO_2:SiO_2/EG:DI Hybrid Nanofluid. *Inventions* 2024:9(1). https://doi.org/10.3390/inventions9010011

[9] Holik M., Živić M., Virag Z., Barac A. Optimization of an organic Rankine cycle constrained by the application of compact heat exchangers. *Energy Convers Manag* 2019:188:333–345. https://doi.org/10.1016/j.enconman.2019.03.039

[10] Faraj A., Faraj J., Harika E., Hachem F., Khaled M. Development of a new method for estimating the overall heat transfer coefficient of heat exchangers – Validation in automotive applications. *Case Studies in Thermal Engineering* 2021:28:101434. https://doi.org/10.1016/j.csite.2021.101434

[11] Albadr J., Tayal S., Alasadi M. Heat transfer through heat exchanger using Al_2O_3 nanofluid at different concentrations. *Case Studies in Thermal Engineering* 2013:1(1):38–44. https://doi.org/10.1016/j.csite.2013.08.004

[12] Kumar N., Sonawane S. S. Experimental study of Fe_2O_3/water and Fe_2O_3/ethylene glycol nanofluid heat transfer enhancement in a shell and tube heat exchanger. *International Communications in Heat and Mass Transfer* 2016:78:277–284. https://doi.org/10.1016/j.icheatmasstransfer.2016.09.009

[13] Mikhienkova E. I., Lysakov S. V., Neverov A. L., Zhigarev V. A., Minakov A. V., Rudyak V. Y. Experimental study on the influence of nanoparticles on oil-based drilling fluid properties. *Journal of Petroleum Science and Engineering* 2022:208. https://doi.org/10.1016/j.petrol.2021.109452

[14] Hussanan A., Salleh M. Z., Khan I., Shafie S. Convection heat transfer in micropolar nanofluids with oxide nanoparticles in water, kerosene and engine oil. *Journal of Molecular Liquids* 2017:229:482–488. https://doi.org/10.1016/j.molliq.2016.12.040

[15] Hong T. K., Yang H. S., Choi C. J. Study of the enhanced thermal conductivity of Fe nanofluids. *J Applied Phys*ics 2005:97(6). https://doi.org/10.1063/1.1861145

[16] Huminic G., Huminic A. Heat transfer characteristics in double tube helical heat exchangers using nanofluids. *Int J Heat Mass Transfer* 2011:54(19–20):4280–4287. https://doi.org/10.1016/j.ijheatmasstransfer.2011.05.017

[17] Asokan N., Gunnasegaran P., Vicki Wanatasanappan V. Experimental investigation on the thermal performance of compact heat exchanger and the rheological properties of low concentration mono and hybrid nanofluids containing Al_2O_3 and CuO nanoparticles. *Thermal Science and Engineering Progress* 2020:20:100727. https://doi.org/10.1016/j.tsep.2020.100727

[18] Khodadadi H., Aghakhani S., Majd H., Kalbasi R., Wongwises S., Afrand M. A comprehensive review on rheological behavior of mono and hybrid nanofluids: Effective parameters and predictive correlations. *International Journal of Heat and Mass Transfer* 2018:127:997–1012. https://doi.org/10.1016/j.ijheatmasstransfer.2018.07.103

[19] Ronewicz K. A. Badania eksperymentalne pierwszego kryzysu wrzenia nanocieczy na poziomych rurkach ze stali nierdzewnej. 2015.

[20] Pavlenko A. Analysis of Methods for Intensifying Heat and Mass Transfer in Liquid Media. *Energies* 2025:18(6):1419. https://doi.org/10.3390/en18061419

[21] Sekrani G., Poncet S. Ethylene- and propylene-glycol based nanofluids: A literature review on their thermophysical properties and thermal performances. *Applied Sciences* 2018:8(11). https://doi.org/10.3390/app8112311

[22] Hussein A. M. Thermal performance and thermal properties of hybrid nanofluid laminar flow in a double pipe heat exchanger. *Exp Therm Fluid Sci* 2017:88:37–45. https://doi.org/10.1016/j.expthermflusci.2017.05.015

[23] MOL. Manufacture of lubricants – MOL Thermol 68. [Online]. [Accessed 13.01.2025]. Available: https://mollubricants.com/en/lubricants-autochemicals/399-industry/industrial-lubricants/heat-transfer-oils/5378-mol-thermol-68/
[24] MOL. Manufacture of lubricants – MOL Thermol 32. [Online]. [Accessed 13.01.2025]. Available: https://mollubricants.com/en/lubricants-autochemicals/industry/industrial-lubricants/heat-transfer-oils/mol-thermol-32/
[25] Patel C. M., Chakraborty M., Murthy Z. V. P. Preparation of fenofibrate nanoparticles by combined stirred media milling and ultrasonication method. *Ultrason Sonochem* 2014:21(3):1100–1107. https://doi.org/10.1016/j.ultsonch.2013.12.001
[26] Sonawane S. S., Khedkar R. S., Wasewar K. L., Rathod A. P. Dispersions of CuO nanoparticles in paraffin prepared by ultrasonication: A potential coolant. In International Conference on Chemical, Biological and Environmental Engineering (IPCBEE), IACSIT Press, 2012.
[27] Gazanfari M. *et al.* Synthesis of aluminium nanoparticles by arc evaporation of an aluminium cathode surfaceю *Bull. Mater. Sci.* 2014:17(4):871–876. https://doi.org/10.1007/s12034-014-0019-0
[28] Fazio E. *et al.* Nanoparticles engineering by pulsed laser ablation in liquids: Concepts and applications. *Nanomaterials* 2020:10(11):2317. https://doi.org/10.3390/nano10112317
[29] Nazarenko O. Nanopowders produced by electrical explosion of wires. In Proceedings of the European Congress of Chemical Engineering (ECCE-6), Copenhagen, 2007.
[30] Bahiraei M., Naghibzadeh S. M., Jamshidmofid M. Efficacy of an eco-friendly nanofluid in a miniature heat exchanger regarding to arrangement of silver nanoparticles. *Energy Convers Manag* 2017:144:224–234. https://doi.org/10.1016/j.enconman.2017.04.076
[31] Ghachem K., Aich W., Kolsi L. Computational analysis of hybrid nanofluid enhanced heat transfer in cross flow micro heat exchanger with rectangular wavy channels. *Case Studies in Thermal Engineering* 2021:24:100822. https://doi.org/10.1016/j.csite.2020.100822
[32] Vallejo J. P., Prado J. I., Lugo L. Hybrid or mono nanofluids for convective heat transfer applications. A critical review of experimental research. *Applied Thermal Engineering* 2022:203:117926. https://doi.org/10.1016/j.applthermaleng.2021.117926
[33] Sidik N. A. C., Adamu I. M., Jamil M. M., Kefayati G. H. R., Mamat R., Najafi G. Recent progress on hybrid nanofluids in heat transfer applications: A comprehensive review. *International Communications in Heat and Mass Transfer* 2016:78:68–79. https://doi.org/10.1016/j.icheatmasstransfer.2016.08.019
[34] Muneeshwaran M., Srinivasan G., Muthukumar P., Wang C. C. Role of hybrid-nanofluid in heat transfer enhancement – A review. *International Communications in Heat and Mass Transfer* 2021:125:105341. https://doi.org/10.1016/j.icheatmasstransfer.2021.105341
[35] Vajjha R. S., Das D. K. Experimental determination of thermal conductivity of three nanofluids and development of new correlations. *Int J Heat Mass Transf* 2009:52(21–22):4675–4682. https://doi.org/10.1016/j.ijheatmasstransfer.2009.06.027
[36] Sundar L. S., Singh M. K., Sousa A. C. M. Enhanced heat transfer and friction factor of MWCNT-Fe_3O_4/water hybrid nanofluids. *International Communications in Heat and Mass Transfer* 2014:52:73–83. https://doi.org/10.1016/j.icheatmasstransfer.2014.01.012
[37] Yu W., Xie H. A review on nanofluids: Preparation, stability mechanisms, and applications. *J Nanomaterials* 2012:1–17. https://doi.org/10.1155/2012/435873
[38] Abadeh A., Mohammadi M., Passandideh-Fard M. Experimental investigation on heat transfer enhancement for a ferrofluid in a helically coiled pipe under constant magnetic field. *J Therm Anal Calorim* 2019:135(2):1069–1079. https://doi.org/10.1007/s10973-018-7478-2
[39] Seth G. S., Kumar R., Tripathi R. Thermo-diffusion effects on the magnetohydrodynamic natural convection flow of a chemically reactive Brinkman type nanofluid in a porous medium. *Bulgarian Chemical Communications* 2019:51(2):168–179. https://doi.org/10.34049/bcc.51.2.4577
[40] Tiwari A. K., Ghosh P., Sarkar J. Investigation of thermal conductivity and viscosity of nanofluids. *J. Environ. Res. Dev.* 2012:7(2).
[41] Rajiv, Kumar H., Sokhal G. S. Effect of different types of nanoparticles on thermophysical properties of water based hybrid nanofluids. *IOP Conf Ser Mater Sci Eng* 2022:1248(1):012071. https://doi.org/10.1088/1757-899X/1248/1/012071
[42] Al-qazzaza A. H. S., Farzaneh-Gorda M., Niazmand H. Systematic analysis with comparison of a chiller plant with horizontal underground heat exchangers and cooling tower. *Journal of Building Engineering* 2024:92:109665. https://doi.org/10.1016/j.jobe.2024.109665
[43] Pandelidis D., Jedlikowski A. Systemy wentylacji i klimatyzacji a energooszczędność. *Inżynier budownictwa*, 2015. [Online]. [Accessed 14.12.2024]. Available: https://inzynierbudownictwa.pl/systemy-wentylacji-i-klimatyzacji-a-energooszczednosc/
[44] de Waard S. J. Shell and Tube Heat Exchanger. licence CC BY-SA 3.0 (https://creativecommons.org/licenses/by-sa/3.0), via Wikimedia Commons. Description added by the author: Dagmara Kotrys-Działak. [Online]. [Accessed

25.04.2025]. Available: https://upload.wikimedia.org/wikipedia/commons/9/9a/Rotterdam_Ahoy_Europort_2011_%2860%29.JPG

[45] Abou Elmaaty T. M., Kabeel A. E., Mahgoub M. Corrugated plate heat exchanger review. *Renewable and Sustainable Energy Reviews* 2017:70:852–860. https://doi.org/10.1016/j.rser.2016.11.266

[46] Gerritse. Plate Heat Exchanger. Dutch Wikipedia, licence CC BY-SA 3.0 (http://creativecommons.org/licenses/by-sa/3.0/), via Wikimedia Commons. Description added by the author: Dagmara Kotrys Działak. [Online]. [Accessed 25.04.2025]. Available: https://upload.wikimedia.org/wikipedia/commons/f/f0/Platenwarmtewisselaar.jpg

[47] Lazarevikj M., Filkoski R. V., Markov Z. CFD analysis of heat transfer and fluid flow in plate heat exchanger with nanofluid. 3rd South East European Conference on Sustainable Development of Energy, Water and Environment Systems – SDEWES SEE 2018 Novi Sad, Serbia, 2018. [Online]. [Accessed 12.12.2024]. Available: https://www.researchgate.net/publication/327013714

[48] Mohammed H. A., Bhaskaran G., Shuaib N. H., Abu-Mulaweh H. I. Influence of nanofluids on parallel flow square microchannel heat exchanger performance. *International Communications in Heat and Mass Transfer* 2011:38(1):1–9. https://doi.org/10.1016/j.icheatmasstransfer.2010.09.007

[49] Wciślik S., Taler D. Economic and Exergy Analysis of TiO2 + SiO2 Ethylene-Glycol-Based Hybrid Nanofluid in Plate Heat Exchange System of Solar Installation. *Energies* 2024:17(13):3107. https://doi.org/10.3390/en17133107

[50] Qi C., Luo T., Liu M., Fan F., Yan Y. Experimental study on the flow and heat transfer characteristics of nanofluids in double-tube heat exchangers based on thermal efficiency assessment. *Energy Convers Manag* 2019:197:111877. https://doi.org/10.1016/j.enconman.2019.111877

[51] El-Maghlany W. M., Hanafy A. A., Hassan A. A., El-Magid M. A. Experimental study of Cu-water nanofluid heat transfer and pressure drop in a horizontal double-tube heat exchanger. *Exp Therm Fluid Sci* 2016:78:100–111. https://doi.org/10.1016/j.expthermflusci.2016.05.015

[52] Javadi F. S. *et al.* The effects of nanofluid on thermophysical properties and heat transfer characteristics of a plate heat exchanger. *International Communications in Heat and Mass Transfer* 2013:44:58–63. https://doi.org/10.1016/j.icheatmasstransfer.2013.03.017

[53] Mukherjee S., Wciślik S., Ebrahim S., Mishra P. C., Ali N. Enhancing cooling performance of a heat exchanger driven by water/alumina-silica hybrid nanofluid: experimental results. *Journal of Enhanced Heat Transfer* 2024:31(2):21–47. https://doi.org/10.1615/JEnhHeatTransf.2023048391

[54] Rashidi M. M., Mahariq I., Alhuyi Nazari M., Accouche O., Bhatti M. M. Comprehensive review on exergy analysis of shell and tube heat exchangers. 2022:147:12301–12311. https://doi.org/10.1007/s10973-022-11478-2

[55] Dąbek L., Kapjor A., Orman Ł. J. Ethyl alcohol boiling heat transfer on multilayer meshed surfaces. *AIP Conference Proceedings* 2016:1745(1):020005. https://doi.org/10.1063/1.4953699

[56] Bialek A., Kargul M., Stokowiec K. Boiling heat transfer on porous single layer brass meshes. *Journal of Physics: Conference Series*, Institute of Physics, 2023. https://doi.org/10.1088/1742-6596/2454/1/012004

[57] Dabek L., Kapjor A., Orman Ł. J. Boiling heat transfer augmentation on surfaces covered with phosphor bronze meshes. *MATEC Web of Conferences*, EDP Sciences, May 2018. https://doi.org/10.1051/matecconf/201816807001

[58] Bialek A., Stokowiec K. Comparison of boiling heat transfer on heaters with mesh structure and microfins. *Journal of Physics: Conference Series*, Institute of Physics, 2023. https://doi.org/10.1088/1742-6596/2454/1/012005

[59] Bahiraei M., Kiani Salmi H., Safaei M. R. Effect of employing a new biological nanofluid containing functionalized graphene nanoplatelets on thermal and hydraulic characteristics of a spiral heat exchanger. *Energy Convers Manag* 2019:180:72–82. https://doi.org/10.1016/j.enconman.2018.10.098

[60] Sundar L. S., Shaik F. Heat transfer and exergy efficiency analysis of 60% water and 40% ethylene glycol mixture diamond nanofluids flow through a shell and helical coil heat exchanger. *International Journal of Thermal Sciences* 2023:184. https://doi.org/10.1016/j.ijthermalsci.2022.107901

[61] Alklaibi A. M., Chandra Mouli K. V. V., Syam Sundar L. Experimental investigation of heat transfer and effectiveness of employing water and ethylene glycol mixture based Fe_3O_4 nanofluid in a shell and helical coil heat exchanger. *Thermal Science and Engineering Progress* 2023:40:101739. https://doi.org/10.1016/j.tsep.2023.101739

[62] Barzegarian R., Aloueyan A., Yousefi T. Thermal performance augmentation using water based Al_2O_3-gamma nanofluid in a horizontal shell and tube heat exchanger under forced circulation. *International Communications in Heat and Mass Transfer* 2017:86:52–59. https://doi.org/10.1016/j.icheatmasstransfer.2017.05.021

[63] Shahrul I. M., Mahbubul I. M., Saidur R., Sabri M. F. M. Experimental investigation on Al_2O_3-W, SiO_2-W and ZnO-W nanofluids and their application in a shell and tube heat exchanger. *International Journal of Heat and Mass Transfer* 2016:97:547–558. https://doi.org/10.1016/j.ijheatmasstransfer.2016.02.016

[64] Hassaan A. M. An investigation for the performance of the using of nanofluids in shell and tube heat exchanger. *International Journal of Thermal Sciences* 2022:177. https://doi.org/10.1016/j.ijthermalsci.2022.107569

[65] Thakur G., Singh G., Thakur M., Kajla S. An experimental study of nanofluids operated shell and tube heat exchanger with air bubble injection. *International Journal of Engineering, Transactions A: Basics* 2018:31(1):136–143. https://doi.org/10.5829/ije.2018.31.01a.19

[66] Dong X., Wu Y., Zhang C., Lu Y., Ma C. Experimental and numerical study on heat transfer and flow characteristics of molten salt nanofluids in spiral-wound tube heat exchanger. *International Journal of Thermal Sciences* 2023:191:108343. https://doi.org/10.1016/j.ijthermalsci.2023.108343

[67] Marzouk S. A., Aljabr A., Almehmadi F. A., Alqaed S., Sharaf M. A. Numerical study of heat transfer, exergy efficiency, and friction factor with nanofluids in a plate heat exchanger. *J Therm Anal Calorim* 2023:148(20):11269–11281. https://doi.org/10.1007/s10973-023-12441-5

[68] Alklaibi A. M., Mouli K. V. V. C., Sundar L. S. Heat transfer, and friction factor of Fe_3O_4–SiO_2/Water hybrid nanofluids in a plate heat exchanger: Experimental and ANN predictions. *International Journal of Thermal Sciences* 2024:195. https://doi.org/10.1016/j.ijthermalsci.2023.108608

[69] Sundar L. S., Punnaiah V., Sharma K. V., Chamkha A. J., Sousa A. C. M. Thermal entropy and exergy efficiency analyses of nanodiamond/water nanofluid flow in a plate heat exchanger. *Diam Relat Mater* 2021:120. https://doi.org/10.1016/j.diamond.2021.108648

[70] Alklaibi A. M., Sundar L. S., Chandra Mouli K. V. V. Experimental investigation on the performance of hybrid Fe3O4 coated MWCNT/Water nanofluidas a coolant of a Plate heat exchanger. *International Journal of Thermal Sciences* 2022:171. https://doi.org/10.1016/j.ijthermalsci.2021.107249

[71] Saleh B., Sundar L. S. Experimental study on heat transfer, friction factor, entropy and exergy efficiency analyses of a corrugated plate heat exchanger using Ni/water nanofluids. *International Journal of Thermal Sciences* 2021:165. https://doi.org/10.1016/j.ijthermalsci.2021.106935

[72] Mohammed H. A., Vuthaluru H. B., Liu S. Thermohydraulic and thermodynamics performance of hybrid nanofluids based parabolic trough solar collector equipped with wavy promoters. *Renewable Energy* 2022:182:401–426. https://doi.org/10.1016/j.renene.2021.09.096

[73] El-Shafay A. S., Mohamed A. M., Ağbulut Ü., Gad M. S., El Maakoul A. Investigation of the effect of magnetic field on the PEC and exergy of heat exchanger filled with two-phase hybrid nanofluid, equipped with an edged twisted tape. *Engineering Analysis with Boundary Elements* 2023:148:153–164. https://doi.org/10.1016/j.enganabound.2022.12.025

[74] Negeed E. S. R., Alhazmy M., Abulkhair H., Attar H. M., Hedia H. S. Numerical simulation of dual-tube heat exchanger equipped with an innovative turbulator containing two-phase hybrid nanofluid: Hydrodynamic and exergy analysis. *Engineering Analysis with Boundary Elements* 2023:155:1059–1068. https://doi.org/10.1016/j.enganabound.2023.07.025

[75] Hussien F. M., Faraj J. J., Hamad A. J. Experimental Investigation of Double Pipe Heat Exchanger Performance based on Alumina and Copper Oxide Working Nanofluids. *IOP Conf Ser Mater Sci Eng* 2021:1105(1):012061. https://doi.org/10.1088/1757-899X/1105/1/012061

[76] Jabłó Nska-Wawrzycka A. *et al.* Ruthenium Complexes with 2-Pyridin-2-yl-1H-benzimidazole as Potential Antimicrobial Agents: Correlation between Chemical Properties and Anti-Biofilm Effects. *International Journal of Molecular Sciences Article Int. J. Mol. Sci* 2021:22(18):10113. https://doi.org/10.3390/ijms221810113

[77] Wciślik S. How Nanofluids May Enhance Energy Efficiency and Carbon Footprint in Buildings? *Sustainability (Switzerland)* 2025:17(15). https://doi.org/10.3390/su17157035